ELSEVIER

Journal of Power Sources 112 (2002) 509–518

JOURNAL OF POWER SOURCES

www.elsevier.com/locate/jpowsour

Performance analysis of molten carbonate fuel cell using a Li/Na electrolyte

H. Morita[a,*], M. Komoda[b], Y. Mugikura[a], Y. Izaki[a], T. Watanabe[a], Y. Masuda[c], T. Matsuyama[c]

[a]*Chemical Energy Engineering Department, Yokosuka Research Laboratory, Central Research Institute of Electric Power Industry, 2-6-1 Nagasaka, Yokosuka 240-0196, Japan*
[b]*Chubu Electric Power Co. Inc., 20-1 Kitasekiyama, Ohdaka-cho, Midori-ku, Nagoya 459-8522, Japan*
[c]*Ishikawajima-Harima Heavy Industries Co. Ltd., 5292 Aioi, Aioi-shi, Hyogo 678-0041, Japan*

Received 27 March 2002; received in revised form 1 July 2002; accepted 13 August 2002

Abstract

Several years ago, Li/Na carbonate (Li_2CO_3/Na_2CO_3) was developed as the electrolyte of molten carbonate fuel cells (MCFCs) in place of the usual Li/K carbonate (Li_2CO_3/K_2CO_3) to the advantage of a higher ionic conductivity and lower rate of cathode NiO dissolution. To estimate the potential of Li/Na carbonate as the MCFC electrolyte, the dependence of the cell performance on the operating conditions and the behavior during long-term performance was investigated in several bench-scale cell operations. The obtained data on the performance of Li/Na cells was analyzed to estimate the impact of voltage losses by using a performance model and discussed in comparison with the data of conventional Li/K cell performance.

Keywords: Molten carbonate fuel cell (MCFC); Li/Na carbonate electrolyte; Cell performance model; Initial and long-term performance

1. Introduction

In molten carbonate fuel cell (MCFC) technology, the progress in terms of improving materials and manufacturing processes is a key to obtain superior cell performance and life. Although various carbonate compositions (the ternary mixtures of Li_2CO_3, Na_2CO_3 and K_2CO_3) were used as the MCFC electrolyte material in early development phases, from the 1950s to the mid-1970s, Li_2CO_3/K_2CO_3 eutectic has been used as the electrolyte in most developments since the mid-1970s [1,2]. In Japan, scientists developing commercial MCFCs also adopted the Li/K carbonate electrolyte for several decades. However, since Yoshioka and Urushibata [3,4] reported about cell performance using a Li/Na carbonate electrolyte an attempt has been made in Japan to change the electrolyte material from Li/K to Li/Na carbonate. Some groups [5–10] also studied the potential of Li/Na carbonate in the early 1990s.

In this study, several Li/Na bench-scale cells were used to understand the dependence of cell performance on various operating conditions (pressure, temperature, current density, gas compositions) and the behavior during long-term performance. The obtained data on Li/Na cell performance is analyzed to estimate the impact of voltage losses (Nernst loss, Ohmic potential drop, anode and cathode polarization) by using a performance model and compared with the data of conventional Li/K cell performance. The aim is to characterize the Li/Na cell performance and contribute towards the design and operation of Li/Na stacks.

2. Experimental

The experimental data of the Li/Na cell performance was obtained by using eight bench-scale cells (No. 1−8). The experimental data of conventional Li/K cell performance to compare with that of Li/Na cell performance was obtained under a contract with NEDO and MCFC Research Association, or collaborative research agreement with CRIEPI and IHI. Table 1 shows the specifications of conventional Li/K cells and the examined Li/Na cells manufactured in IHI. The specifications of Li/K and Li/Na cells in terms of anode, cathode and current collector are similar, whereas the specifications of Li/Na cells in terms of thickness and structure

* Corresponding author. Tel.: +81-468-56-2121; fax: +81-468-56-3346.
E-mail address: morita@criepi.denken.or.jp (H. Morita).

0378-7753/02/$ – see front matter
PII: S0378-7753(02)00468-8

Nomenclature

List of symbols

a, c_1, c_2	optimum parameters of R_a and R_c determined by experimental data
A_i	frequency factor for resistance parameters R_{ir}, a, c_1 and c_2 determined by Arrhenius plot
E	open circuit voltage (V)
(I, J)	ordered pair for representing the coordinates of separate sections in the cell
J	current density (A/cm^2)
$M(\ )$	gas concentration (mol fraction)
$P(\ )$	partial pressure of anode hydrogen, cathode oxygen and carbon dioxide (atm)
R	gas constant (J/(mol K))
R_a, R_c	anode, cathode reaction resistance (Ω cm^2)
R_{ir}	internal resistance (Ω cm^2)
t	operating time (h)
T	temperature (K)
V	output (uniform) voltage (V)

Greek letters

ΔH_i	apparent activation energy for resistance parameters determined by Arrhenius plot (J/mol)
η_{ne}	Nernst loss (V)

of the γ-$LiAlO_2$ matrix differ from cell to cell. The thicknesses are approx. 0.9 mm (cell No. 1, 2), 0.7 mm (cell No. 3, 4) and 1.0 mm (cell No. 5–8). The structures consist of both, coarse and fine particles (conventional type), and fine and uniform particles (advanced type II).

Both the experiments of Li/K and Li/Na cells were carried out using several pieces of test equipments designed for running bench-scale cell, which can operate the cell up to a temperature of 720 °C and a pressure of 7.00 atm. Anode and cathode gas was each controlled by a mass-flow meter (H_2, CO_2, N_2, O_2 and air). If necessary, the controlled gas mixtures were humidified at the temperature of the bubbling vessel, and fed into the cell. Open circuit voltage (OCV), output voltage and internal resistance (IR) were measured at various temperatures (575–700 °C) and pressures (1.00–5.00 atm) in order to understand the dependence of the cell performance on the operating conditions. The output voltage was generally measured at 150 mA/cm^2, and the IR was calculated as the resistance of the OCV under a frequency of 1 kHz using the mΩ m, Hewlett-Packard 4338A. After the measurements for understanding the dependence of the cell performance on the operating conditions were completed, each cell was operated under a pressurized condition more than 5000 h to investigate the behavior during long-term performance.

After the long-term operation, the cell was cooled down to room temperature and disassembled to carry out the post-test analyses of the components. In the post-test, the cross-sections of the matrix and the corrosion layer formed between the electrode and the current collector were studied by using a scanning electron microscope (SEM). The amount of deposited Ni in the matrix, which is caused by the dissolution of the NiO in the cathode, was determined by using an inductively coupled plasma (ICP) atomic emission spectrometer.

3. MCFC performance model description

Fig. 1 shows the performance curves of MCFC under the practical operational range in current density. A linear relationship between the current density and the output voltage is found in the experimental curve. Regarding the linear range, the following potential balance must be satisfied approximately in the cell:

$$V \cong E - \eta_{ne} - (R_{ir} + R_a + R_c)J \quad (1)$$

where V is the output (uniform) voltage, E the equilibrium cell voltage (i.e. open circuit voltage), η_{ne} the Nernst loss, R_{ir} the internal resistance, R_a and R_c the anode and cathode reaction resistances due to the polarization in the respective electrodes and J the current density. In order to take the effect of the current distribution into account, the potential balance expressed in Eq. (1) is calculated in every separate cell section where the current distribution seems to be uniform, and so Eq. (1) reduces to Eq. (2) in every section:

$$V = E(\mathrm{I,J}) - \{R_{ir} + R_a(\mathrm{I,J}) + R_c(\mathrm{I,J})\}J(\mathrm{I,J}) \quad (2)$$

where ordered pair (I,J) represents the coordinates of separate cell sections. The degree of (I,J) is generally adopted between the (5 × 5) and (10 × 10) on this calculation. The effect of the Nernst loss is included in the local equilibrium voltage E(I,J) of Eq. (2), which is calculated in the Nernst

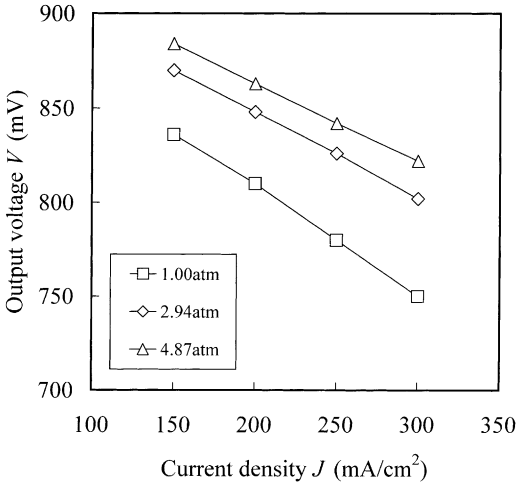

Fig. 1. Performance curves of Li/Na cell (No. 1) at several pressures, temperature = 650 °C; fuel H_2/CO_2 = 80/20% (20% humidification), utilization = 80%; oxidant air/CO_2 = 70/30%, utilization = 40%.

Table 1
Specifications of bench-scale Li/K and Li/Na cells

Cell	Cell flame area (mm)	Cell flame material	Electrode area (cm^2)	Anode/cathode current collector	Anode	Cathode	Electrolyte matrix	Thickness of matrix (mm)	Electrolyte Li_2CO_3/K_2CO_3 (%)	Electrolyte Li_2CO_3/Na_2CO_3 (%)
Li/K (10 cells[a])	160 × 160	Aluminized SUS316L	108	Ni201/ SUS316L	Ni–4% Al, Cr	in situ NiO (Ni–3% $MgCO_3$)	γ-$LiAlO_2$ (conventional type) + Al_2O_3 fiber	0.9	70/30	60/40
Li/Na cell										
No. 1, 2	150 × 150	Aluminized SUS 310S	110	Ni201/ SUS316L	Ni–4% Al, Cr	in situ NiO (Ni–3% $MgCO_3$)	γ-$LiAlO_2$ (conventional type) + Al_2O_3 fiber	0.9		60/40
No. 3, 4	150 × 150	Aluminized SUS 310S	110	Ni201/ SUS316L	Ni–4% Al, Cr	in situ NiO (Ni–3% $MgCO_3$)	γ-$LiAlO_2$ (advanced type II) + Al_2O_3 fiber	0.7		60/40
No. 5, 6	150 × 150	Aluminized SUS 310S	110	Ni201/ SUS316L	Ni–4% Al, Cr	in situ NiO (Ni–3% $MgCO_3$)	γ-$LiAlO_2$ (advanced type II) + $LiAlO_2$ fiber	1.0		57/43
No. 7, 8	150 × 150	Aluminized SUS 310S	110	Ni201/ SUS316L	Ni–4% Al, Cr	in situ NiO (Ni–3% $MgCO_3$)	γ-$LiAlO_2$ (advanced type II) + Al_2O_3 fiber	1.0		60/40

[a] Cell No. P4–P6 and L9–L15.

equation. The Nernst equation takes account of the gas composition distribution from the inlet to the outlet of the anode and cathode. The calculation of the R_a, R_c and J distribution is also based on the gas composition and utilization, whereas the distribution of R_{ir} in the bench-scale cell is not taken into account and regarded as a constant. R_{ir} is regarded as a function of temperature only, and the temperature of the bench-scale cell is uniform in experiments. The calculation procedure, which takes account of the distribution, was described previously [11]. According to Eqs. (4) and (5) [12,13], the expressions R_a and R_c are assumed to be functions of the reactant partial pressures:

$$R_{ir}(T) = A_{ir} \exp\left(\frac{\Delta H_{ir}}{RT}\right) \tag{3}$$

$$R_a(T) = a(T)P(H_2)^{-0.5} = A_a \exp\left(\frac{\Delta H_a}{RT}\right)P(H_2)^{-0.5} \tag{4}$$

$$\begin{aligned} R_c(T) &= c_1(T)P(O_2)^{-0.75}P(CO_2)^{0.5} + c_2(T)M(CO_2)^{-1.0} \\ &= A_{c1} \exp\left(\frac{\Delta H_{c1}}{RT}\right)P(O_2)^{-0.75}P(CO_2)^{0.5} \\ &\quad + A_{c2} \exp\left(\frac{\Delta H_{c2}}{RT}\right)M(CO_2)^{-1.0} \end{aligned} \tag{5}$$

Here, the ordered pair (I,J) of the reactant partial pressure is omitted in Eqs. (4) and (5). Eq. (5) expresses the cathode reaction resistance which has the most impact when estimating the MCFC performance. It is derived from the reactant partial pressure based on a simultaneous diffusion mechanism of superoxide ions (O_2^-) and CO_2 in the melt [14–16]. Because the experimental data of each resistance at varying temperatures shows good linearity on Arrhenius plots, the temperature dependence of each resistance is determined by the Arrhenius type equation as shown in Eqs. (3)–(5). The a, c_1 and c_2 in Eqs. (4) and (5) are optimum parameters in each cell. They are determined by using the optimum method to minimize the objective function between the experimental output voltages obtained from the several gas conditions [17] and the calculated output voltages of Eq. (2). In the calculation for minimizing the objective function, the final value of the average error between experimental and calculated output voltages is converged within ±5 mV. Once the values R_{ir}, a, c_1, and c_2 have been determined, it is possible to estimate the voltage losses caused by the Nernst loss, the internal resistance and the anode and cathode reaction resistances of Eq. (1) under various operating conditions.

4. Results and discussion

4.1. Cell performance under a 1.00 atm and 650 °C condition

Li/Na carbonate has the advantages of higher ionic conductivity, lower rate of cathode dissolution and lower

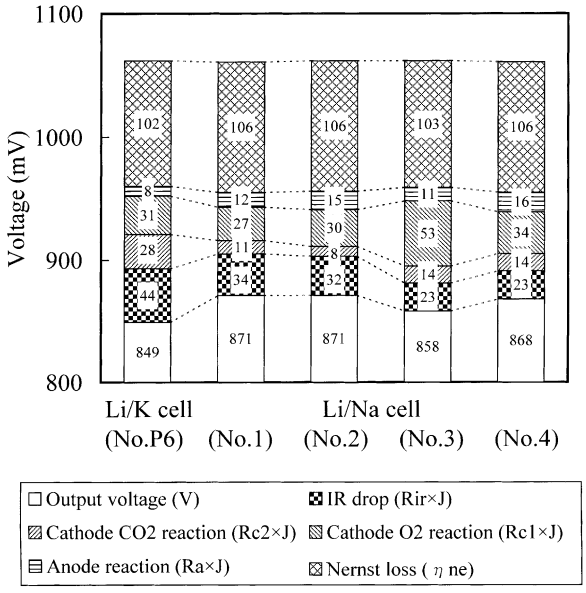

Fig. 2. Analysis of Li/K and Li/Na cell performance under atmospheric condition, pressure = 1.00 atm; temperature = 650 °C; current density = 150 mA/cm^2; fuel H_2/CO_2 = 80/20% (20% humidification), utilization = 60%; oxidant air/CO_2 = 70/30%, utilization = 40%. Matrix thickness of Li/K cell = 0.9 mm, Li/Na cell = 0.9 or 0.7 mm (Table 1).

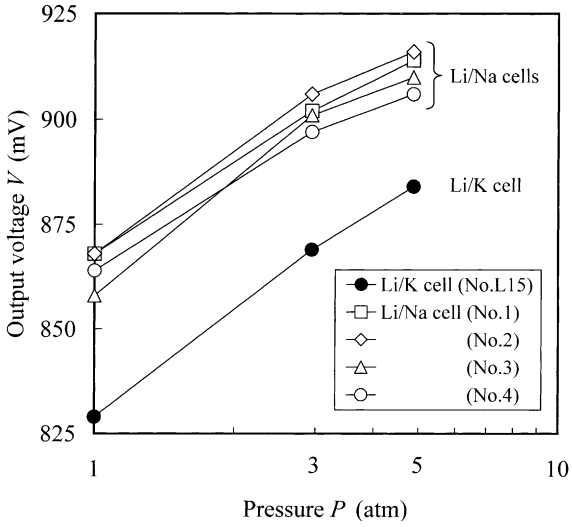

Fig. 3. Dependence of the cell voltage on the operating pressure, temperature = 650 °C; current density = 150 mA/cm^2; fuel H_2/CO_2 = 80/20% (20–30% humidification), utilization = 60%; oxidant air/CO_2 = 70/30%, utilization = 40%.

electrolyte vapor loss than Li/K carbonate, whereas Li/Na carbonate has the disadvantage of lower oxygen gas solubility [1,18]. In order to clarify the potential of the Li/Na carbonate as the MCFC electrolyte, the examinations of the Li/Na cell performance were carried out under the following for a MCFC bench-scale cell typical conditions: 1.00 atm pressure, 650 °C temperature, 150 mA/cm^2 current density, H_2/CO_2 = 80/20% (20% humidification), 60% utilization as anode gas and air/CO_2 = 70/30%, 40% utilization as cathode gas. Fig. 2 shows the analysis of Li/K and Li/Na cell performance under this operating condition. The analysis is based on the values of the performance model, R_{ir}, a, c_1 and c_2, which are determined by the experimental data of output voltages at several gas compositions. All Li/Na cells are superior in their output voltage to the Li/K cell, which performed best amongst the conventional Li/K cells. In view of analyzing the cell performance according to the model, the lower internal resistance and the lower cathode reaction resistance of carbon dioxide, which corresponds to the c_2 parameter in Eq. (5), contribute towards the superior performance of the Li/Na cell. The different levels of voltage loss caused by the internal resistance in Li/K and Li/Na cells can be explained by the different values of ionic conductivity of the Li/K (∼1.65/(Ω cm)) and Li/Na (∼2.40/(Ω cm)) carbonate melts [18]. However, the different levels of voltage loss caused by the cathode carbon dioxide reaction resistance are still not defined very well by the reaction mechanism. Regarding the different levels of voltage loss caused by the cathode oxygen, which corresponds to the c_1 parameter in Eq. (5), the performance does not seem to differ in Li/K and Li/Na cells (approx. 30 mV), except Li/Na cell No. 3 (53 mV). The fact possibly reflects that Li/Na carbonate does not always have the disadvantage of a lower oxygen gas solubility than Li/K carbonate in practical Li/Na cells.

4.2. Pressure and temperature effects on cell performance

Fig. 3 shows the dependence of the cell voltage on the operating pressure in Li/K and Li/Na cells. Li/Na cell performance is superior to average Li/K cell performance at any pressure. The reason for the superior performance of Li/Na cells is due to the lower internal resistance and the lower cathode carbon dioxide reaction resistance described in the preceding chapter. Based on the resistance parameters, which are determined by the output voltage data at the respective pressure levels, Fig. 4 shows the analysis of the effect pressure has on the Li/K and Li/Na cell performance. The reason for the increase of output voltage by putting the MCFC under pressure is mainly due to two factors regardless of the cell type. One is the increase in open circuit voltage based on the Nernst equation, the other is the decrease in cathode oxygen reaction resistance, which corresponds to the partial pressure dependence of the c_1 parameter (i.e. $P(O_2)^{-0.75}P(CO_2)^{0.5}$) in Eq. (5).

Fig. 5 shows the dependence of the cell voltage on the operating temperature in Li/K and Li/Na cells. Generally, the Li/Na cell performance is superior to the average Li/K cell performance at any temperature. However, the voltage drop of the Li/Na cells in relation to the decreasing temperature is larger than that of the average Li/K cell. Especially, the voltage drop in Li/Na cell No. 3, which indicates large voltage loss caused by the cathode oxygen (53 mV) as shown in Fig. 2, is very large compared to the other Li/Na

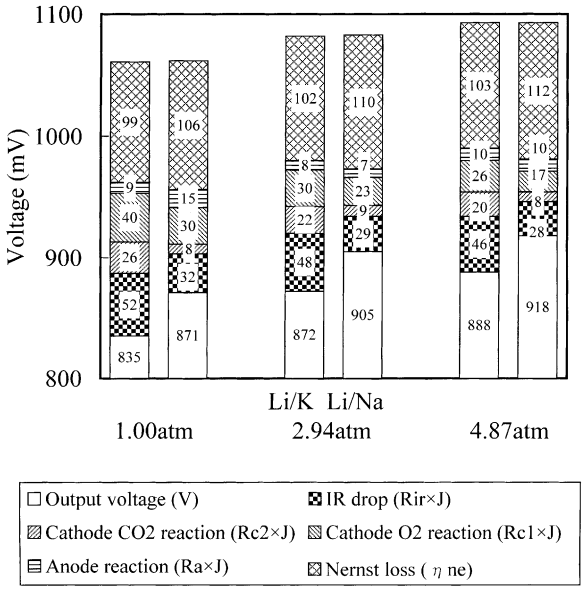

Fig. 4. Analysis of the effect pressure on Li/K (No. L15) and Li/Na (No. 2) cell performance, temperature = 650 °C; current density = 150 mA/cm^2; fuel H_2/CO_2 = 80/20% (20% humidification), utilization = 60%; oxidant air/CO_2 = 70/30%, utilization = 40%.

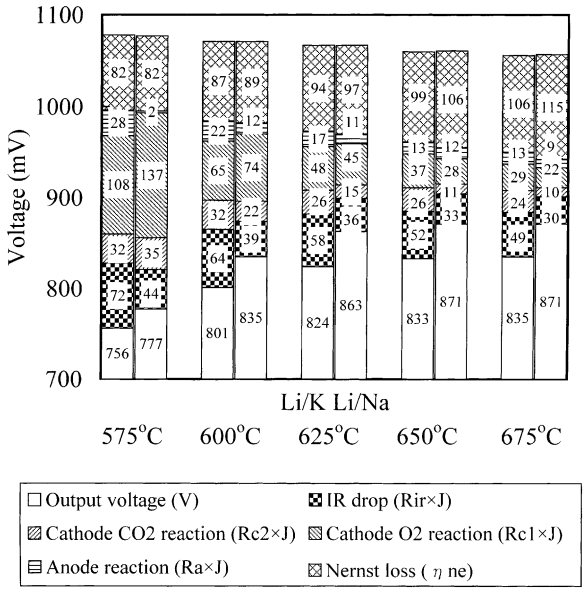

Fig. 6. Analysis of the effect temperature on Li/K (No. L13) and Li/Na (No. 1) cell performance, pressure = 1.00 atm; current density = 150 mA/cm^2; fuel H_2/CO_2 = 80/20% (20% humidification), utilization = 60%; oxidant air/CO_2 = 70/30%, utilization = 40%.

cells examined. Regarding the large voltage loss in Li/Na cell No. 3, however, the performance is improved to be equivalent to the other cell performances as the operating pressure is increased. The reason for the improvement in cell No. 3 would be the increase in oxygen solubility in the melt due to the increased operating pressure. Therefore, the large voltage drop, which is due to the lower oxygen solubility in the Li/Na carbonate melt, possibly occurs as decreasing operating temperature under atmospheric operation in the Li/Na cell. Fig. 6 shows the analysis of the effect

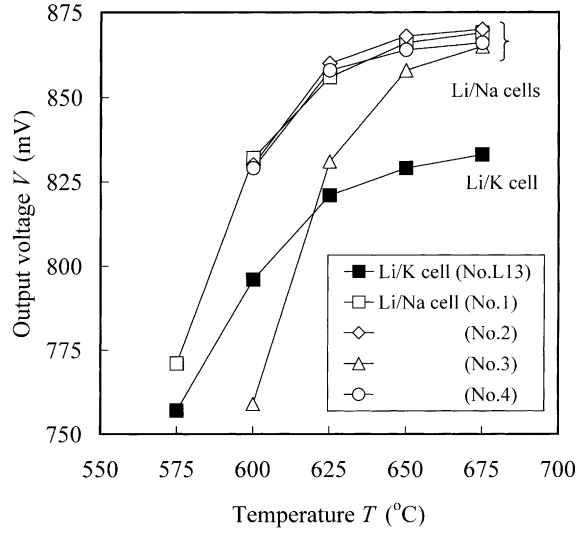

Fig. 5. Dependence of the cell voltage on the operating temperature, pressure = 1.00 atm; current density = 150 mA/cm^2; fuel H_2/CO_2 = 80/20% (20% humidification), utilization = 60%; oxidant air/CO_2 = 70/30%, utilization = 40%.

temperature has on the Li/K and Li/Na cell performance based on the resistance parameters, which are determined by the output voltage data at respective temperatures. In this figure, the Li/Na cell No. 1, which shows a standard performance as shown in Fig. 5, is compared with the Li/K cell. As the operating temperature increases, the open circuit voltage (E) and the Nernst loss (η_{ne}) in Eq. (1) decrease and increase respectively to function as the negative factor of the MCFC performance (i.e. output voltage V), whereas the internal resistance (R_{ir}) and the anode and cathode reaction resistances (R_a and R_c) in Eq. (1) decrease to function as the positive factor. According to the balance of factors above, it is probable that there is not a gain of output voltage beyond a temperature of 650 °C regardless of the cell type. The result suggests that there is not advantage in the state-of-the-art technology to operate MCFCs beyond 650 °C. Regarding the gain of each resistance (R_{ir}, R_a and R_c) in relation to operating temperature, the gain of internal resistance and cathode reaction resistance of oxygen, which corresponds to the c_1 parameter, are large and therefore dominant factors of temperature. Regarding the dominant factors, the voltage drop due to the cathode reaction resistance of oxygen mainly decides on the performance of the MCFC under lower temperatures (≤600 °C). This is a remarkable feature on Li/Na cells. The frequency factor and the activation energy of the parameters in Li/K and Li/Na cells obtained from the Arrhenius plots (575–700 °C) are shown in Table 2. These values correspond to the frequency factor (A_i) and activation energy (ΔH_i) in Eqs. (3)–(5). Regarding the Arrhenius plot of the anode reaction resistance parameter (a) in Eq. (4), the degree of linearity in the plot is poor, amongst Li/Na cells in particular, and the temperature

Table 2
Frequency factor and activation energy of the parameters in Li/K and Li/Na cells obtained from the Arrhenius plots (575–700 °C)

	A_{ir}	ΔH_{ir} (kJ/mol)	A_a	ΔH_a (kJ/mol)	A_{c1}	ΔH_{c1} (kJ/mol)	A_{c2}	ΔH_{c2} (kJ/mol)
Li/K cells ($L = 0.9$ mm)								
Average of 10 cells	1.28×10^{-2}	25.2	1.39×10^{-6}	77.8	1.97×10^{-6}	83.4	2.20×10^{-3}	22.8
Li/Na cell								
No. 1 ($L = 0.9$)	9.84×10^{-3}	23.8	2.15×10^{-3}	21.8	5.78×10^{-9}	126	1.67×10^{-7}	89.7
No. 2 ($L = 0.9$)	1.46×10^{-2}	20.3	7.27×10^{-3}	13.8	3.08×10^{-9}	131	7.57×10^{-5}	41.1
No. 3 ($L = 0.7$)	2.96×10^{-3}	30.7	–	–	5.80×10^{-10}	148	3.01×10^{-10}	140
No. 4 ($L = 0.7$)	9.66×10^{-3}	21.2	8.66×10^{-4}	31.1	4.31×10^{-8}	112	6.43×10^{-5}	45.7
No. 5 ($L = 1.0$)	1.00×10^{-2}	25.8	–	–	5.50×10^{-10}	145	5.25×10^{-5}	45.8
No. 6 ($L = 1.0$)	4.91×10^{-2}	16.0	1.27×10^{-3}	28.0	5.04×10^{-9}	130	1.18×10^{-4}	40.4
Average (geometric mean)	(1.12×10^{-2})	23.0	2.04×10^{-3}	23.7	3.28×10^{-9}	132	3.39×10^{-6}	67.1

L: matrix thickness, (–): poor degree of linearity in Arrhenius plots, ( ): the value under no consideration of matrix thickness.

dependence of parameter a in the Li/Na cell is small enough to be a constant.

4.3. Long-term performance due to continuous operations

In this chapter, the effects of electrolyte material, current density and steam in the cathode are discussed according to the results of the continuous operations more than 5000 h. In order to clarify the factors of voltage decay in relation to operating time, the performance model described in Chapter 3 is extended by the operating time. In the extended model [17], the output voltage decay according to time is expressed by Eq. (6). There is an increase in the values R_{ir}, R_a and R_c with time (t).

$$V(t) = E - \eta_{ne} - (R_{ir}(t) + R_a(t) + R_c(t))J \quad (6)$$

The increase in the values R_a and R_c corresponds to the increase in the values a, c_1 and c_2 in Eq. (7).

$$R_a(t) = a(t)P(H_2)^{-0.5}$$
$$R_c(t) = c_1(t)P(O_2)^{-0.75}P(CO_2)^{0.5} + c_2(t)M(CO_2)^{-1.0} \quad (7)$$

Therefore, the factor voltage decay to operating time is analyzed by measuring and estimating variations in the values R_{ir}, and a, c_1 and c_2 to operating time.

4.3.1. Effect of electrolyte material

The effect of electrolyte material is classified into two. One is the effect of electrolyte composition (i.e. Li/K or Li/Na carbonate), the other is that of matrix structure (i.e. conventional or advanced type as shown in Table 1).

Fig. 7 shows the long-term performance of Li/K and Li/Na cells, which is manufactured with a conventional matrix type. These voltage decay rates of Li/K and Li/Na cells at 5000 h are 7.1 and 7.2 mV/1000 h, respectively, as shown in Table 3 (a) and (b). The values are almost equal. Therefore, it is probable that there is not difference between Li/K and Li/Na cells in the effect of the electrolyte compositions regarding the voltage decay rate. Fig. 8 shows the analysis of Li/Na cell No. 1 performance to operating time, as shown in Fig. 7.

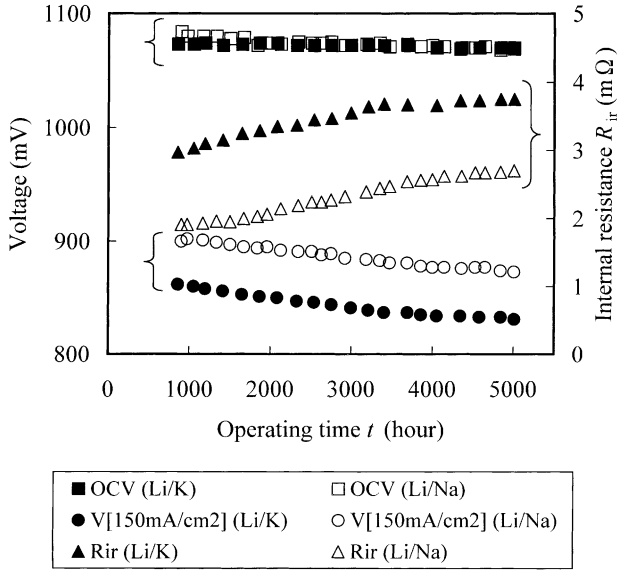

Fig. 7. Long-term performance of Li/K (No. $L15$) and Li/Na (No. 1) cells with a conventional matrix, pressure = 2.94 atm; temperature = 650 °C; current density = 150 mA/cm^2; fuel H_2/CO_2 = 80/20% (20% humidification), utilization = 60%; oxidant air/CO_2 = 70/30%, utilization = 40%.

Here, the relation of the performance to the operating time is obtained by inserting variations of the values R_{ir}, a, c_1 and c_2. Regarding the voltage decay factors, the values R_{ir} and R_c (i.e. c_1 and c_2 parameters) increase with time to degrade the cell performance, whereas R_a is almost a constant to time. This trend is generally observed during the continuous operation of bench-scale cells under a cathode dry condition (air/CO_2), regardless of the cell type.

Table 3 (d) shows the voltage decay rate of Li/Na cell No. 3, which is manufactured with an advanced matrix type. The value of cell No. 3 at 5000 h shows 4.2 mV/1000 h, which is superior to that of Li/Na cell No. 1 with a conventional matrix type as shown in Table 3 (b). Regarding the trend of the voltage decay, the variations in the values R_{ir} and R_c are also the dominant factors influencing the voltage decay as the trend of Fig. 8, however, the degree of the variations is improved compared with the result of Fig. 8.

Table 3
Continuous operating condition and voltage decay rate at each cell operated 650 °C

Cell No.	Matrix type	Total operating time (h)	Pressure (atm)	Current density (mA/cm^2)	Cathode gas	Voltage decay rate at 5000 h (mV/1000 h)
(a) Li/K cell No. L15	Conventional	5,000	2.94	150	Dry cond.	7.1
(b) Li/Na cell No. 1	Conventional	5,000	2.94	150	Dry cond.	7.2
(c) Li/Na cell No. 2	Conventional	5,000	2.94	300	Dry cond.	13.3
(d) Li/Na cell No. 3	Advanced II	8,000	2.94	150	Dry cond.	4.2
(e) Li/Na cell No. 5	Advanced II	17,500	4.87	150	Wet cond.	2.9

Anode gas: $H_2/CO_2 = 80/20\%$ (20–30% humidification), utilization = 60%; cathode gas dry cond.: air/$CO_2 = 70/30\%$, O_2/CO_2 utilization = 40/40%; cathode gas wet cond.: $O_2/CO_2/N_2 = 8/12/80\%$ (13% humidification), O_2/CO_2 utilization = 25/35%.

This improvement (~3 mV/1000 h) between (b) and (d) in Table 3 is probably achieved by changing the $LiAlO_2$ matrix structure from mixed coarse and fine particles (conventional type) to fine and uniform particles (advanced type II).

4.3.2. Effect of current density

The MCFC development in Japan will try to increase the power density of MCFCs by increasing current density from the present value of 150 mA/cm^2 to a higher value (~250 mA/cm^2). Therefore, the examination of long-term performance under a high current density was carried out to estimate the effect the current density has on the voltage decay during long-term operation. Table 3 (c) shows the voltage decay rate of Li/Na cell No. 2, which has the same specification to cell No. 1 as shown in Table 1, under high current density. The value of cell No. 2 at 5000 h shows 13.3 mV/1000 h under a condition of 300 mA/cm^2. This result is in proportion with the value of the current density and about twice as high as cell No. 1 under a condition of 150 mA/cm^2 as shown in Table 3 (b). Since the operating conditions of cell nos. 1 and 2 are the same, except the current density and the gas flow rate corresponding to the value of current density, the difference of the voltage decay rates results from that of the current density only in Eq. (6). In fact, the behavior of internal resistance (R_{ir}) and reaction resistance ($R_a + R_c$) in relation to operating time is very similar in cell nos. 1 and 2 as shown in Fig. 9. Therefore, the current density has no effect on the increase in cell resistances to operating time. The fact that the gas flow rate is also independent of the increasing cell resistances probably reflects that the effect of the electrolyte loss caused by the vaporization does not contribute towards the factor voltage decay in practical Li/Na cells.

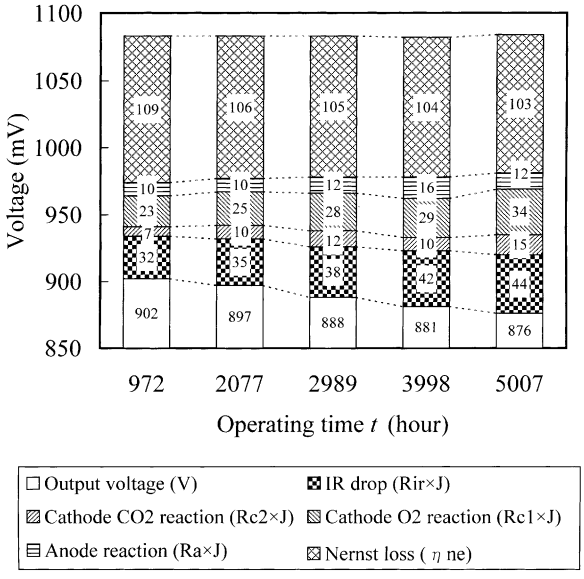

Fig. 8. Analysis of Li/Na cell (No. 1) performance to operating time, pressure = 2.94 atm; temperature = 650 °C; current density = 150 mA/cm^2; fuel $H_2/CO_2 = 80/20\%$ (20% humidification), utilization = 60%; oxidant air/$CO_2 = 70/30\%$, utilization = 40%.

4.3.3. Effect of steam in cathode

The previous results of the bench-scale cell examinations mainly discussed the long-term performance of MCFCs under the cathode dry gas condition (air/$CO_2 = 70/30\%$), which has been adopted in Japan as a typical gas condition for estimating a bench-scale cell performance at each development phase. However, the cathode wet gas condition, which includes approx. 10% steam, needs to be adopted as the prospective gas condition for commercial MCFC plants. The reason is that the cathode CO_2 gas is supplied

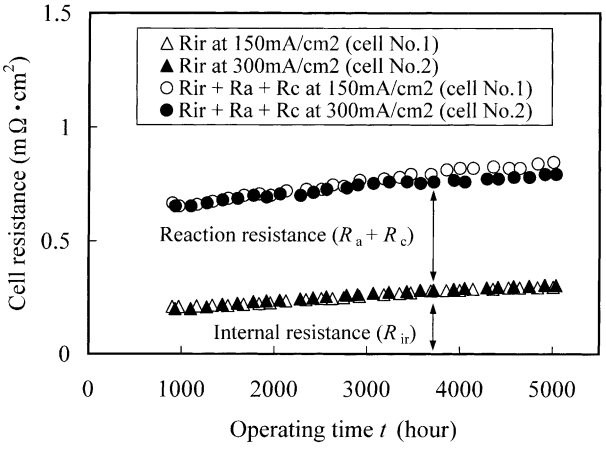

Fig. 9. Comparison of effect the 150 and 300 mA/cm^2 operations on the cell resistance history, pressure = 2.94 atm; temperature = 650 °C; current density = 150 or 300 mA/cm^2; fuel $H_2/CO_2 = 80/20\%$ (20% humidification), utilization = 60%; oxidant air/$CO_2 = 70/30\%$, utilization = 40%.

to the MCFC stack through the CO_2 recirculation by burning the anode exhaust gas (H_2, CO_2, CO, H_2O) in the catalytic burner of the natural gas reformer on the level of the MCFC power plant. Therefore, it is necessary to carry out the examination of long-term performance under the cathode wet gas condition in order to estimate the long-term performance of commercial MCFC power plants. The cathode wet gas condition for estimating the MCFC performance was adopted as follows:

$$O_2/CO_2/N_2 = 8/12/80\% \ (13\% \ \text{humidification}),$$
$$O_2/CO_2 \ \text{gas utilization} = 25/35\%$$

The cathode gas condition above refers to the condition of a 1000 kW class power plant at Kawagoe power station of Chubu Electric Power Co. Inc. in Japan [19,20].

Table 3 (e) shows the voltage decay rate of Li/Na cell No. 5 with an advanced matrix under the cathode wet gas condition. The value of cell No. 5 at 5000 h shows 2.9 mV/1000 h under a condition of 150 mA/cm^2, which is superior to that of cell No. 3 under the cathode dry condition as shown in Table (d). This improvement (∼1 mV/1000 h) between (d) and (e) in Table 3 is probably achieved by the effect of steam in the cathode. The factors voltage decay are generally the variations of the values R_{ir}, c_1 and c_2 under the cathode dry condition as observed in Fig. 8, whereas the factors voltage decay are the variations of the values R_{ir} and c_1 only under the cathode wet gas condition, and the variation of the value c_2 corresponds with the cathode reaction resistance of carbon dioxide is not perceived. The effect the cathode steam has on the stability of the c_2 parameter towards the operating time is confirmed in the operation of other cells, regardless of the cell type [21]. However, the problem regarding the effect of cathode steam is still not fully solved and the subject requires further study.

4.4. Prospective behavior of long-term performance in commercial MCFC stack

The electrolyte loss caused due to corrosion on the metal component of MCFCs, which is the main factor of voltage decay in MCFCs, is generally classified into two types. One is the inside loss which is caused by the corrosion of parts of the current collector and the corrugated plate, the other is the outside loss which is caused by the corrosion of part of the cell flame. According to Urushibata et al. [22], the volume of the outside loss decreases as the cell size increases from a bench-scale cell (∼100 cm^2) to a stack-scale cell (∼1 m^2) and becomes almost negligible compared to that of inside loss in the stack-scale cell. In view of their analysis regarding the electrolyte loss, the voltage decay rate of the stack is expected to be smaller than that of the bench-scale cell by the decrease in the outside loss. Therefore, the long-term operation of a bench-scale cell, which makes the electrolyte loss as small as possible, is necessary to estimate the behavior of long-term performance on the stack-scale cell level.

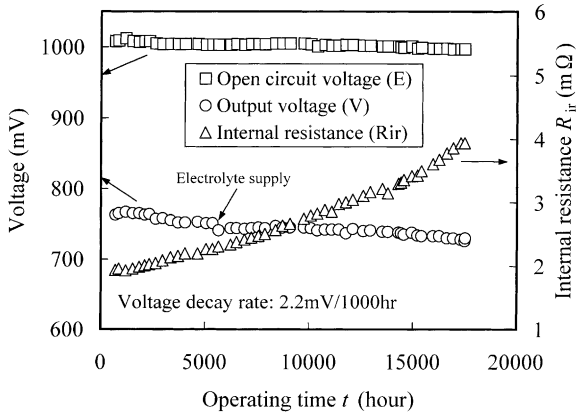

Fig. 10. Long-term performance of Li/Na cell (No. AL2) with an advanced matrix under wet cathode gas condition, pressure = 1.00 atm; temperature = 625 °C; current density = 150 mA/cm^2; fuel H_2/CO_2 = 80/20% (20% humidification), utilization = 60%; oxidant $O_2/CO_2/N_2$ = 8/12/80% (13% humidification), O_2/CO_2 utilization = 25/35%.

Fig. 10 shows the long-term performance of a cell under such a condition, which has been carried out under a contract with NEDO/MCFC Research Association. Although the cell's specifications are similar to those of cell No. 5, as shown in Table 1, a pipe for supplying the carbonate to the cell in operation is installed at its cell flame and its operating temperature is lower than 650 °C in order to restrain the electrolyte loss in the cell. The carbonate was added to the operating cell at approx. 5000 h. The voltage decay rate of this cell at 17,500 h shows 2.2 mV/1000 h under a condition

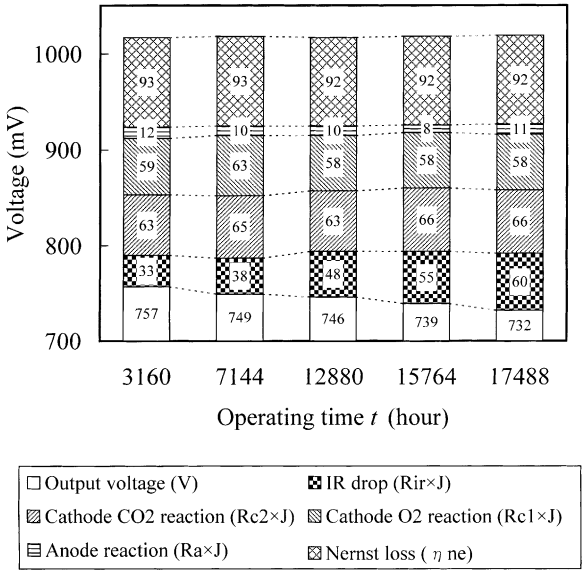

Fig. 11. Analysis of Li/Na cell (No. AL2) performance to operating time under wet cathode gas condition, pressure = 1.00 atm; temperature = 625 °C; current density = 150 mA/cm^2; fuel H_2/CO_2 = 80/20% (20% humidification), utilization = 60%; oxidant $O_2/CO_2/N_2$ = 8/12/80% (13% humidification), O_2/CO_2 utilization = 25/35%.

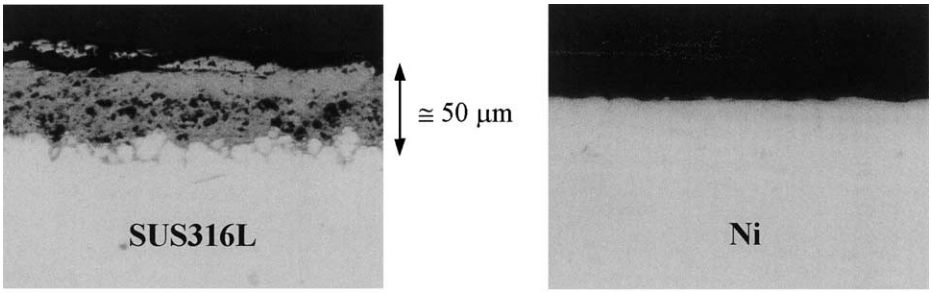

Fig. 12. SEM photograph of the cathode and anode current collector cross-sections after 17,500 h continuous operation at 650 °C (Li/Na cell No. 5).

of 625 °C and 150 mA/cm^2, which is a very low value on bench-scale cell level beyond 15,000 h. Fig. 11 shows the relation of this cell performance to operating time, which is obtained by varying the values R_{ir}, a, c_1 and c_2. The factor voltage decay is mainly the increase of R_{ir}, and the increase of the other parameters (a, c_1 and c_2) cannot be perceived. The result of Fig. 11 suggests that the factor voltage decay in the stack-scale cell is almost the increase in the value R_{ir}. Regarding the increase in the value R_{ir}, there is a factor independent of the amount of electrolyte in the cell, because the increased rate R_{ir} in Fig. 10 does not change before or after the addition of carbonate at approx. 5000 h. A main factor for this constant variation in R_{ir} would be the increase in the resistance due to the corrosion layer on the current collector as mentioned in the following chapter.

4.5. Post-test analysis

The amount of electrolyte loss caused by the corrosion on current collector occupies a large amount of the inside loss to be a main factor of the constant variation in R_{ir} to the operating time even on the stack-scale cell, because the amount of electrolyte loss per unit area of current collector is independent of the cell size. Fig. 12 shows a SEM photograph of the cathode and anode current collector cross-sections in Li/Na cell No. 5 after 17,500 h operation. The anode side current collector made of Ni is not penetrated by the corrosion of molten carbonate even after operating for 17,500 h, whereas the cathode side current collector made of SUS316L is penetrated forming a corrosion layer approx. 50 μm thick. Based on the observations by SEM, the degree of the corrosion thickness on cathode current collector in Li/Na cells was similar to that of the corrosion thickness in Li/K cells, and a difference between the penetration of corrosion in Li/K and Li/Na cells cannot be perceived. Therefore, a key to improve the voltage decay caused by the increase of R_{ir} would be to prevent the penetration of the corrosion in the cathode current collector during long-term operation, regardless of the cell type.

Regarding the amount of Ni in relation to the operating time, the amount in Li/Na cells was seemed to be about half as much as in Li/K cells based on the analyses by ICP.

5. Conclusions

In view of the Li/Na bench-scale cell operations to understand the dependence of cell performance on various operating conditions and the behavior during long-term performance, the following conclusions have been obtained.

1. Any examined Li/Na cell performance is superior in output voltage to the Li/K cell performance under a condition of 1.00 atm and 650 °C. The reason for the superior performance of the Li/Na cell is the lower internal resistance and the lower cathode reaction resistance of carbon dioxide.
2. The temperature dependence of Li/Na cells under atmospheric conditions is larger than that of Li/K cells, because the oxygen solubility in Li/Na carbonate is lower. Therefore, the operation of Li/Na cells under atmospheric pressure and lower temperatures (≤600 °C) possibly run the risk of a large voltage drop.
3. Voltage decay rate in long-term operation is similar between Li/K and Li/Na cells, and the difference in the voltage decay rate between Li/K and Li/Na electrolytes cannot be perceivable. The voltage decay rate increases in proportion to the current density, and the effect the current density has on the increase of the cell resistance in relation to the operating time cannot be perceivable.
4. As a result of the long-term operation in bench-scale cell, which makes the electrolyte loss as small as possible in order to estimate the behavior of long-term performance on stack-scale cell level, the voltage decay is mainly caused by the increase of internal resistance. The corrosion layer on the cathode current collector made of stainless steel mainly contributes towards the increase of internal resistance. Therefore, a key to improve the voltage decay in commercial MCFC stacks would be to prevent the penetration the corrosion on the cathode current collector during long-term operation.

Acknowledgements

This work was carried out as a collaborative research agreement with Chubu Electric Power, CRIEPI and IHI.

Some of the data used in this paper was quoted from the results of bench-scale cell operations under a contract with New Energy and Industrial Technology Development Organization (NEDO) and the MCFC Research Association (Technology Research Association for Molten Carbonate Fuel Cell Power Generation System). The authors appreciate the advice and support they received.

References

[1] J.R. Selman, H.C. Maru, L.G. Marianowski, E. Ong, A. Pigeaud, V. Sampath, Advances in Molten Salt Chemistry, in: G. Mamantov, J. Braunstein, C.B. Mamantov (Eds.), vol. 4, Plenum Press, New York, 1981.
[2] J.R. Selman, Fuel Cell Systems, in: Leo J.M.J. Blomen, Michael N. Mugerwa (Eds.), Plenum Press, New York, 1993.
[3] S. Yoshioka, H. Urushibata, Denki Kagaku (presently Electrochemistry) 64 (1996) 909.
[4] S. Yoshioka, H. Urushibata, Denki Kagaku (presently Electrochemistry) 64 (1996) 1074.
[5] K. Tanimoto, Y. Miyazaki, M. Yanagida, S. Tanase, T. Kojima, H. Ohtori, H. Okuyama, T. Kodama, Int. J. Hydrogen Energy 17 (1992) 821.
[6] P. Tomczyk, G. Mordarski, J. Electroanal. Chem. 304 (1991) 85.
[7] L.K. Bieniasz, J. Electroanal. Chem. 304 (1991) 101.
[8] P. Tomczyk, L.K. Bieniasz, J. Electroanal. Chem. 304 (1991) 111.
[9] G. Mordarski, J. Electroanal. Chem. 304 (1991) 123.
[10] L.K. Bieniasz, P. Tomczyk, J. Electroanal. Chem. 353 (1993) 195.
[11] Y. Mugikura, T. Abe, T. Watanabe, Y. Izaki, Development of a Correlation Equation for the Performance of MCFC, CRIEPI Rep-EW91002, 1991.
[12] H. Morita, Y. Mugikura, Y. Izaki, T. Watanabe, T. Abe, Denki Kagaku (presently Electrochemistry) 65 (1997) 740.
[13] H. Morita, Y. Mugikura, Y. Izaki, T. Watanabe, T. Abe, J. Electrochem. Soc. 145 (1998) 1511.
[14] K. Yamada, T. Nishina, I. Uchida, J.R. Selman, Electrochim. Acta 38 (1993) 2405.
[15] T. Nishina, I. Uchida, J.R. Selman, J. Electrochem. Soc. 141 (1994) 1191.
[16] K. Yamada, T. Nishina, I. Uchida, Electrochim. Acta 40 (1995) 1927.
[17] H. Morita, Y. Mugikura, Y. Izaki, T. Watanabe, T. IEE Jpn. 120-B (2000) 1112.
[18] C. Sishtla, R. Donado, E. Ong, R. Remick, Carbonate fuel cell technology IV, in: J.R. Selman, I. Uchida, H. Wendt, D.A. Shores, T.F. Fuller (Eds.), Proceedings of the Electrochemical Society, vol. 97 (4), Pennington, NJ, USA, 1997, 315 pp.
[19] M. Iio, M. Komoda, Y. Esaki, Fuel Cell Seminar Abstracts, 1998, 158.
[20] T. Mihama, T. Kahara, M. Takeuchi, S. Takashima, in: Proceedings of the 3rd FCDIC Fuel Cell Symposium, FCDIC, Tokyo, Japan, 1996, 109 pp.
[21] H. Morita, M. Yoshikawa, Y. Mugikura, Y. Izaki, T. Watanabe, in: Proceedings of the 5th FCDIC Fuel Cell Symposium Proceedings, FCDIC, Tokyo, Japan, 1998, 261 pp.
[22] H. Urushibata, Y. Fujita, T. Nishimura, S. Yoshioka, Denki Kagaku (presently Electrochemistry) 65 (1997) 121.